RL66 a second-generation curcumin analog has potent *in vivo* and *in vitro* anticancer activity in ER-negative breast cancer models

BABASAHEB YADAV[1], SEBASTIEN TAURIN[1], LESLEY LARSEN[2] and RHONDA J. ROSENGREN[1]

Departments of [1]Pharmacology and Toxicology, [2]Chemistry, University of Otago, Dunedin, New Zealand

Received June 3, 2012; Accepted July 30, 2012

DOI: 10.3892/ijo.2012.1625

Abstract. There is a need for the development of new safe and efficacious drug therapies for the treatment of estrogen receptor (ER)-negative breast cancers. 1-Methyl-3,5-bis[(E)-4-pyridyl) methylidene]-4-piperidone (RL66) is a second generation curcumin analog that exhibits potent cytotoxicity towards a variety of ER-negative breast cancer cells. Therefore, we have further examined the mechanism of this novel drug in *in vitro* and *in vivo* models of ER-negative breast cancer. The mechanistic studies demonstrated that RL66 (2 μM) induced cell cycle arrest in the G2/M phase of the cell cycle. Moreover, RL66 (2 μM) caused 40% of SKBr3 cells to undergo apoptosis after 48 h and this effect was time-dependent. This correlated with an increase in cleaved caspase-3 as shown by western blot analysis. RL66 (2 μM) also decreased HER2/neu phosphorylation and increased p27 in SKBr3 cells, while in MDA-MB-231 and MDA-MB-468 cells RL66 (2 μM) significantly decreased Akt phosphorylation and transiently increased the stress kinases JNK1/2 and MAPK p38. In addition, RL66 exhibited anti-angiogenic potential *in vitro* as it inhibited HUVEC cell migration 46% and the ability of these cells to form tube-like networks. RL66 (8.5 mg/kg) suppressed the growth of MDA-MB-468 xenograft tumors by 48% compared to vehicle control following 10 weeks of daily oral administration. Microvessel density in the tumors from treated mice was also decreased 57% compared to control. Thus our findings demonstrate that RL66 has potent proapoptotic and anti-angiogenic properties *in vivo* and *in vitro* and has the potential to be further developed as a drug for the treatment of ER-negative breast cancer.

Correspondence to: Dr Rhonda J. Rosengren, Department of Pharmacology and Toxicology, 18 Frederick Street, University of Otago, Dunedin 9016, New Zealand
E-mail: rhonda.rosengren@otago.ac.nz

Abbreviations: RL66, 1-methyl-3,5-bis[(E)-4-pyridyl)methylidene]-4-piperidone; ER, estrogen receptor; TNBC, triple negative breast cancer

Key words: triple negative breast cancer, angiogenesis, MDA-MB-468, xenograft, HER2

Introduction

Breast cancer is the most prevalent form of cancer diagnosed in women, and there continues to be limited drug treatment options for the ~30% of patients with estrogen receptor (ER)-negative breast cancer (1,2). In the search for effective drugs for ER-negative breast cancer, several lead compounds from natural products have emerged including curcumin (diferuloylmethane), the primary bioactive compound isolated from the rhizome of turmeric (*Curcuma longa* Linn.). Curcumin has numerous pharmacological, chemopreventative and chemotherapeutic actions, and *in vitro* studies have also demonstrated that curcumin exhibits potent cytoxicity toward numerous cell lines including ER-negative human breast cancer cells (3-9). Furthermore, *in vivo* studies have demonstrated decreased tumorigenesis of many organs, including the mammary gland (10-15). However, curcumin has shown limited clinical efficacy, due to its low bioavailability and low stability (11). Therefore, numerous groups have concentrated on improving drug efficacy, bioavailability and stability by synthesizing analogs of curcumin. Specifically, cyclohexanone analogs of curcumin have shown enhanced activity and stability compared to curcumin (16). Specifically, the cyclohexanone-containing curcumin derivative 2,6-bis((3-methoxy-4-hydroxyphenyl)methylene)-cyclohexanone (BMHPC) was cytotoxic towards ER-negative breast cancer cells (IC_{50} of 5.0 μM) (17), although bioavailability and *in vivo* efficacy were still problematic. More recently the fluorinated cyclohexanone derivative EF24 has shown potent cytotoxicity toward MDA-MB-231 cells with an IC_{50} value of 0.8 μM (18,19).

Our laboratory has been involved in the search for new drug treatments for ER-negative breast cancer and we have shown that 2nd generation heterocyclic cyclohexanone curcumin analogs exhibit potent cytotoxicity toward ER-negative breast cancer cells. This work demonstrated that 1-methyl-3,5-bis[(E)-4-pyridyl)methylidene]-4-piperidone (RL66) (Fig. 1) exhibited IC_{50} values of 0.8, 0.5 and 0.6 μM for MDA-MB-231, MDA-MB-468 and SKBr3 breast cancer cells, respectively (20). It also induced apoptosis, as ~18% of MDA-MB-231 cells underwent apoptosis after 12 h of RL66 treatment (2 μM) (20). Only one other compound synthesized (RL71) showed a more potent effect *in vitro* (21), but this compound did not suppress tumor growth *in vivo*. Therefore, this study was designed to comprehensively investigate the potency and mechanisms of action of RL66 *in vitro* and *in vivo* in order to determine its potential to be developed into a drug for ER-negative breast cancer.

Materials and methods

Materials. HUVEC, MDA-MB-231, MDA-MB-468 and SKBr3 cells were purchased from American Type Culture Collection (Manassas, VA, USA). Primary antibodies to NF-κB, p38, pp38, NF-κB, JNK, pJNK, cleaved caspase-3, 4EBP1, p4EBP1, p27, mTOR, pmTOR, HER2, pHER2 and β-actin were purchased from Cell Signaling Technology (Danvers, MA, USA). Akt and pAkt primary antibodies were purchased from BD Biosciences (Auckland, New Zealand). Dulbecco's modified Eagle's medium (DMEM) nutrient mixture Ham's F-12, sulforhodamine B salt, propidium iodide (PI), ammonium persulfate, horseradish peroxidase were purchased from Sigma-Aldrich (Auckland, New Zealand). Acrylamide, bisacrylamide, sodium dodecylsulfate and PVDF membrane were purchased from Bio-Rad Laboratories (Hercules, CA, USA). Complete mini EDTA-free protease inhibitor cocktail and Annexin V-FLUOS were purchased from Roche Diagnostics Corporation (Mannheim, Germany). RL66 was prepared as described previously (18). All other chemicals were of the highest purity commercially available.

Cell maintenance. MDA-MB-231, MDA-MB-468 and SKBr3 cells were maintained in complete growth media composed of DMEM/Ham's F12 supplemented with 5% fetal bovine serum (FBS), 2 mM L-glutamine, 100 U/ml streptomycin, 250 ng/ml amphotericin B, and 100 U/ml penicillin and 2.2 g/l $NaHCO_3$.

Cytotoxicity. MDA-MB-231, MDA-MB-468 and SKBr3 cells ($95x10^4$ cells/well) were seeded in 12-well plates in 1 ml DMEM/HamF12 supplemented with 5% FBS, 100 U/ml penicillin, 100 μg/ml streptomycin, 25 ng/ml amphotericin B and 2.2 g/l $NaHCO_3$ and incubated for 24 h at 37˚C. To determine cytotoxicity over a time-course, cells were treated with RL66 (1.5 or 2 μM) for 6, 12, 24, 36, 48 and 72 h. Vehicle control cells were treated with DMSO (0.1%). Cell number in each well was determined using the sulforhodamine B (SRB) assay (22).

Cell cycle analysis. Flow cytometry was used to analyze DNA content in order to determine cell cycle distribution. MDA-MB-231, MDA-MB-468 and SKBr3 cells were plated and treated with RL66 (1.5 or 2 μM) or 0.1% DMSO as control for 6-48 h in 6-well plates. The cells were harvested, washed with PBS and then fixed in 70% ethanol. Following rehydration with PBS, the cells were stained with PI in the dark at 4˚C as described (23). The samples were analyzed via flow cytometry using a FACSCalibur flow cytometer (BD Biosciences). The percentage of cells in each phase of cell cycle was determined using Cell Quest Pro software. Results are expressed as percent of cells in each phase of the cell cycle.

Induction of apoptosis. MDA-MB-468, and SKBr3 cells were seeded in 6-well culture plate in 2 ml of DMEM/HamF12 supplemented with 5% FBS, 100 U/ml penicillin, 100 μl/ml streptomycin, 25 ng/ml amphotericin B and 2.2 g/l $NaHCO_3$. The cells were treated with RL66 (1.5 or 2 μM) or vehicle control for 12-36 h. Apoptosis was assessed using Annexin V-FLUCOS/PI staining, as described (24). The samples were analyzed using a FACSCalibur flow cytometer (BD Biosciences) and the proportion of apoptotic cells was determined using CellQuest Pro software.

Preparation of cell lysates. MDA-MB-231, MDA-MB-468 and SKBr3 cells were seeded in 10-cm culture dishes at $2.5x10^6$ cells per well in 10 ml of DMEM/HamF12 supplemented with 5% FBS, 100 U/ml penicillin, 100 μg/ml streptomycin, 25 ng/ml amphotericin B and 2.2 g/l $NaHCO_3$. Cells were treated with RL66 (2 or 3 μM) or vehicle control for 0-36 h. At the end of treatment, whole cell lysates were prepared and protein concentration of the lysates was determined using the bicinchoninic acid (BCA) method (25).

Western blot analysis. Cell lysates were resolved by SDS-PAGE (40 μg protein per well) and then the proteins were transferred to a PVDF membrane. Protein levels were analyzed with the desired primary antibodies, followed by horseradish peroxidase-conjugated secondary antibodies (Bio-Rad Laboratories). The digital chemiluminescence images were taken by a Versadoc densitometer (Bio-Rad Laboratories).

Transwell migration. Transwell migration was performed using 24-well plates containing BioCoat™ Matrigel™ Invasion Chamber inserts (BD Biosciences, Bedford, MA, USA). HUVEC cells (50,000/well) were plated on rehydrated Matrigel coated culture inserts. The bottom chamber contained 500 μl of EGM serum free media. The cells were treated with 0.1% DMSO or RL66 (1 μM) and incubated for 18 h at 37˚C in a humidified 5% CO_2 incubator. After incubation, all contents from well inserts were aspirated and non-migrated cells were removed with a cotton swab. Migrated cells on the bottom of the filters were stained with DiffQuick solution for 1 min and excess stain was washed with water and dried. Cells on the filters were counted using a Zeiss Axioplan camera and compared to the control well insert that contained no matrigel. Results are expressed as migrated cells as a percent of total cell population.

Endothelial tube formation. Geltrex matrigel (125 μl) was added onto 24-well plates which was then incubated at 37˚C, 5% CO_2 for 30 min. HUVEC cells ($5x10^4$/well) were loaded into each well, followed by addition of DMSO (0.1%) or RL66 (1 μM). The plate was incubated at 37˚C, 5% CO_2 for 18 h and photos (x200) were taken by an individual blinded to the treatment groups.

Animals and housing. Female CD-1 mice (6-week-old) were purchased from the Hercus Taieri Resource Unit (Dunedin, New Zealand). All procedures were approved by the University of Otago (AEC no. 91/07). Mice were housed in pathogen-free conditions with woodchip bedding with access to food (Reliance rodent diet, Dunedin, NZ) and water *ad libitum*. Mice were housed in a 21-24˚C environment on a scheduled 12 h light/dark cycle and acclimatized for 3 days prior to experimentation.

MDA-MB-468 xenografts. Female CD1 athymic nude mice (5-6-week-old) were purchased from Hercus Taieri Resource Unit. They were maintained at 21-24˚C with a 12-h light/dark cycle in a specifically designed pathogen-free isolation facility and allowed to acclimatize for 1 week before experimentation. Mice were inoculated into the right flank with MDA-MB-468 cells ($2x10^6$/50 μl matrigel), which were left to form palpable tumors. Tumor volume was measured weekly with electronic calipers (L x W x H). When the tumor volume reached approximately 100 mm^3, mice (5/group) were randomly assigned to the

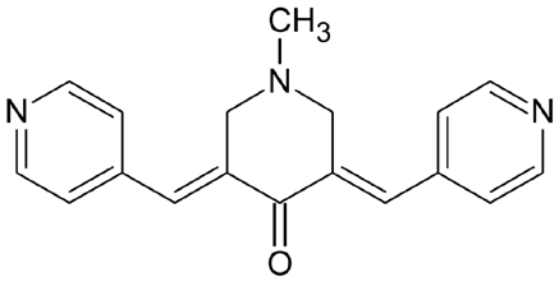

Figure 1. Chemical structure of RL66.

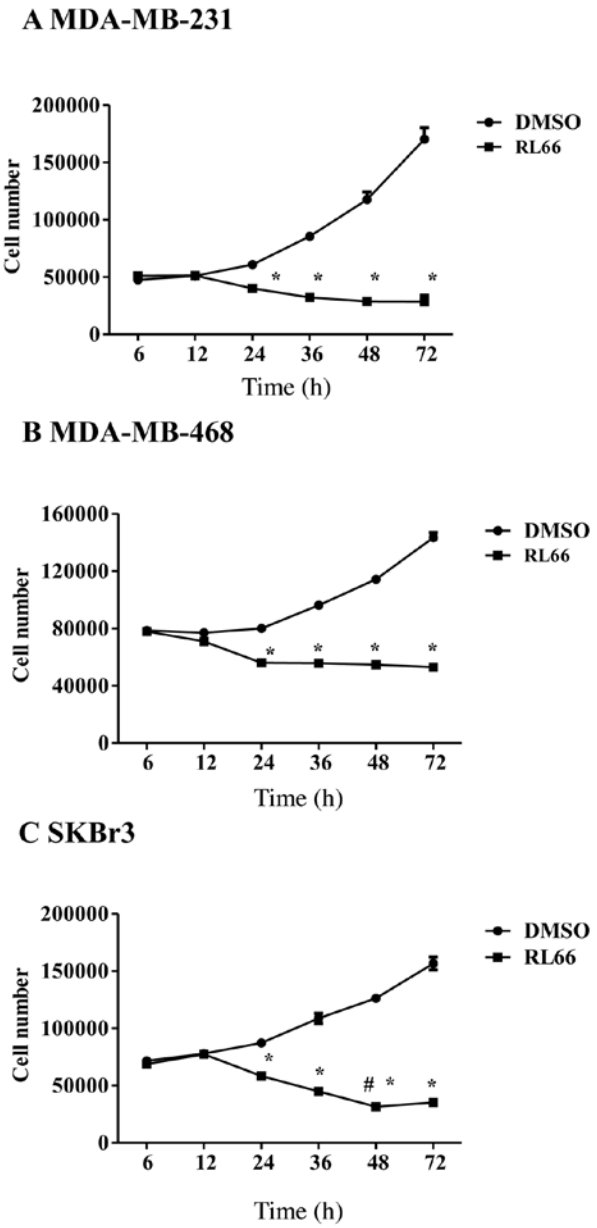

Figure 2. Time-course cytotoxicity of RL66 in (A) MDA-MB-231, (B) MDA-MB-468 and (C) SKBr3 cells. Cells were treated with either RL66 (2 μM) or DMSO (0.1 %) for 6-72 h. Cell number was determined using the SRB assay. Each symbol represents the mean ± SEM of 3 independent experiments performed in triplicate. The data were analyzed using a two-way ANOVA coupled with a Bonferroni post hoc test where asterisc indicates a statistically significant difference compared with the control group, $p<0.001$. [#]indicates a statistically significant difference compared with all previous time points, $p<0.01$.

various treatment groups. Mice were then orally gavaged with RL66 (0.85 or 8.5 mg/kg/day), or water as the vehicle control (5 ml/kg/day) for 10 weeks. Dosing solutions were prepared fresh each day.

Assessment of animal health. Food consumption and body weight were monitored daily throughout the treatment period. Mice were euthanized by CO_2 inhalation 24 h following the last dose and necropsies were then performed. Blood was collected via the inferior vena cava and placed on ice, while major organs, as well as tumors were excised and weighed. Organ weights are expressed as a percentage of body weight. Plasma was separated and used to determine hepatotoxicity via the plasma marker alanine aminotransferase (ALT) activity using a commercially available kit (Medica Pacifica, Auckland, New Zealand). Results are expressed as IU/l.

Immunohistochemistry of tumor sections. Tumors were embedded in OCT compound and then sectioned (12 mm), fixed in acetone, and air-dried overnight. Sections were then washed twice in Tween-20 PBS, incubated with normal serum for 30 min at room temperature, and then incubated overnight with primary CD105 antibody. Slides were then rinsed and peroxidase blocked using hydrogen peroxide (3%) before incubation with the appropriate secondary antibody for 30 min at room temperature in a humidified chamber. The sections were then incubated with ExtrAvidin (Bio-Rad Laboratories, Auckland, New Zealand) (1:20) for 30 min at room temperature in a humidified chamber before development with 3,30-diaminobenzidine tetrahydrochloride as the chromogen and counterstaining with Mayer's haematoxylin. Once slides were dehydrated, DPX mounting medium and coverslips were applied. The sections were analyzed from tumors obtained from each mouse and a representative slide is shown in the results section.

Statistical analysis. All time course data were analyzed using a two-way ANOVA coupled with a Bonferroni post hoc test. Tumor volume was analyzed using a repeated measures 2-way ANOVA coupled with a Bonferroni post hoc test. For all data in which time was not a factor, the data were analyzed using a one-way ANOVA coupled with a Bonferroni post hoc test. $p<0.05$ was the minimum requirement for a statistically significant difference.

Results

Previously we have shown that RL66 elicited sub micromolar IC_{50} values in three different ER-negative breast cancer cell lines (20). Therefore, the first aim of this study was to examine the time-course of RL66-mediated cytotoxicity toward MDA-MB-231, MDA-MB-468 and SKBr3 cells. The results showed that RL66 elicited time-dependent and cell line-dependent cytotoxicity (Fig. 2A-C). Specifically, time-dependent cytotoxicity was elicited in SKBr3 cells where 2 μM signficantly increased cytotoxicity at 48 h compared with all previous time points (Fig. 2C). However, in the two TNBC cell lines no further cytotoxicity was elicited after 24 h. Thus, RL66 showed potent cytotoxicity toward SKBr3 cells compared to a cytostatic effect in TNBC cells.

We next examined whether the cytotoxicity of RL66 was due to cell cycle arrest. Treatment of MDA-MB-231,

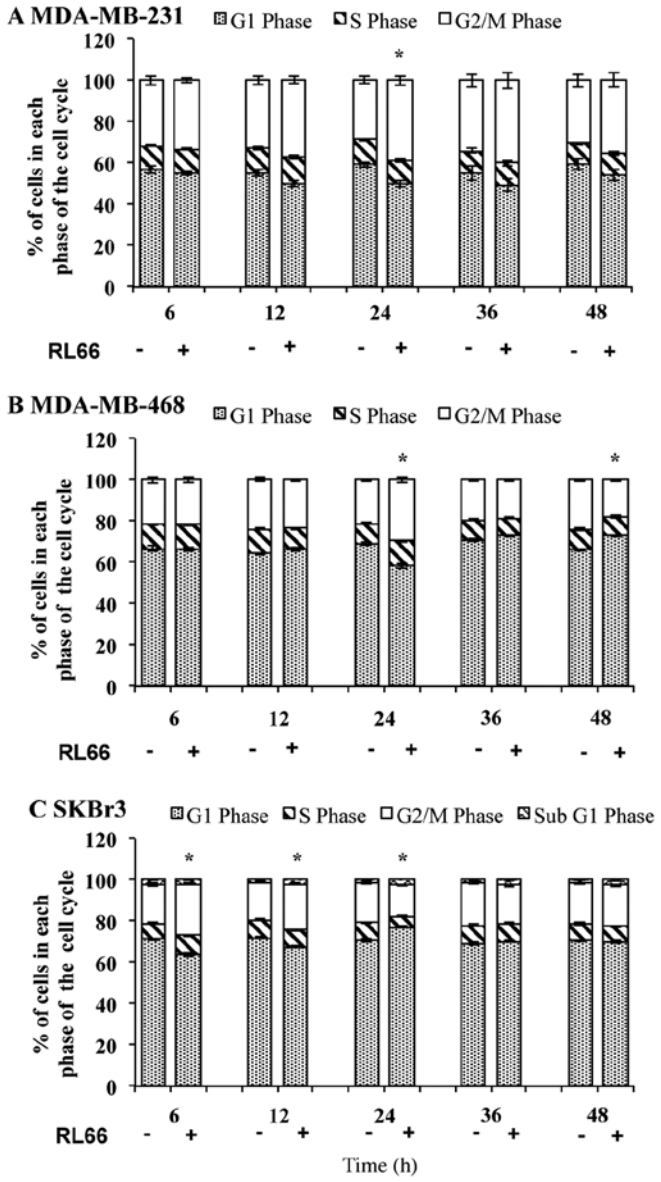

Figure 3. Cell cycle arrest following treatment of ER negative breast cancer cells with RL66 in (A) MDA-MB-231, (B) MDA-MB-468 and (C) SKBr3 cells. Cells were treated with RL66 (2 μM) for 6, 12, 24, 36 and 48 h. Vehicle control cells were treated with 0.1 % DMSO. Propidium iodide staining and flow cytometry was used to determine the proportion of cells in the various phases of the cell cycle. Columns represent the mean proportion of cells in each phase of cell cycle (percentage of total) ± SEM of 3 independent experiments conducted in triplicate. Data were analyzed with a two-way ANOVA coupled with a Bonferroni post hoc test. *indicates a statistically significant difference between treatment and control in the number of cells in the G2/M phase of the cell cycle, p<0.001. #indicates a statistically significant difference in the number of cells in the G2/M phase of the cell cycle compared with all other time points, p<0.01.

MDA-MB-468, and SKBr3 cells with RL66 produced G2/M phase arrest in all three cell lines. Specifically, at 24 h, RL66 caused an 150% increase in the proportion of G2/M phase cells over control in both MDA-MB-231 (Fig. 3A) and MDA-MB-468 cells (Fig. 3B). In SKBr3 cells, after 6 and 12 h, the proportion of cells undergoing G2/M phase was increased by 130 and 120%, respectively, compared to control (Fig. 3C). Moreover, there was a significant reduction in the proportion of cells in S phase at 24 h. SKBr3 cells were also the only cell type to show an increase in subG1 cells.

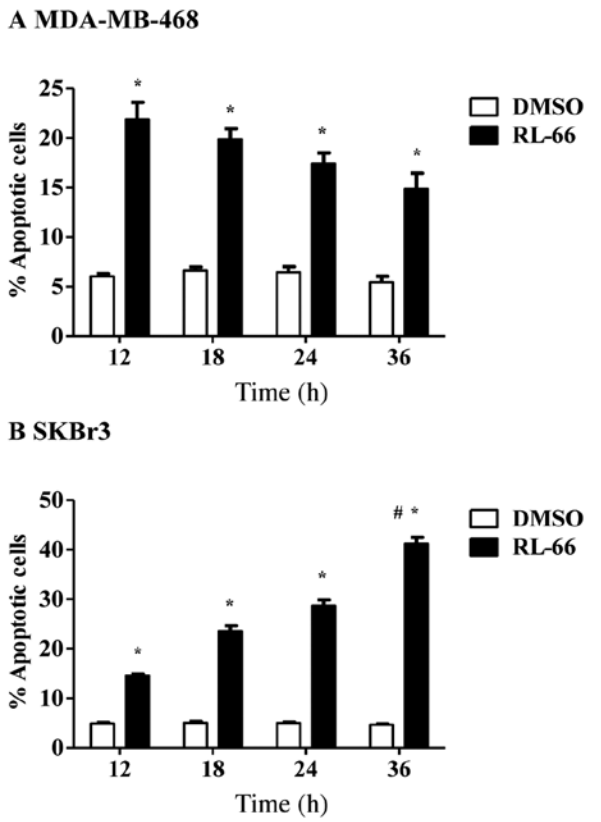

Figure 4. Induction of apoptosis following treatment of (A) MDA-MB-468 and (B) SKBr3 cells with RL66. Cells were treated with RL66 (2 μM) for 12, 18, 24, 36 h. Vehicle control cells were treated with 0.1 % DMSO. Values are expressed as mean number of apoptotic cells as a percentage of the total population ± SEM from 3 independent experiments conducted in triplicate. Data were analyzed using a two-way ANOVA coupled with a Bonferroni post hoc test. *indicates a statistically significant difference compared with the control group, p<0.001. #indicates a statistically significant difference compared with all previous time points, p<0.01.

To determine if RL66-mediated cell cycle arrest resulted in apoptosis, time-dependent changes in apoptosis were examined. The induction of apoptosis was time-dependent in SKBr3 cells, as 42% of cells were apoptotic after 36 h and this was significantly elevated compared to all other time points (Fig. 4B). In contrast 15-22% of MDA-MB-468 cells underwent apoptosis and this effect was maintained from 12-36 h (Fig. 4A) indicating the lack of a time-dependent effect. G2/M arrest did not drive apoptosis in MDA-MB-468 cells, as apoptosis was increased at 12 h, which was prior to the increase in G2/M phase arrest. However, the early appearance of G2/M phase arrest at 6 h in SKBr3 cells is a likely reason why these cells show a strong apoptotic response over time. Our previous work with RL66 in MDA-MB-231 cells indicated that the induction of apoptosis was weakest in this cell line, as 18% of cells underwent apoptosis and this decreased to 8% after 18-36 h (20). Overall RL66 displayed a more potent cytotoxic effect in SKBr3 cells. To determine if this was due to the inhibition of HER2/neu expression, drug-mediated changes in HER2/neu and other downstream cell signaling proteins were determined via western blot analysis.

Treatment of SKBr3 cells with RL66 (2 μM) decreased the ratio of pHER2/HER2, with an almost complete inhibition for

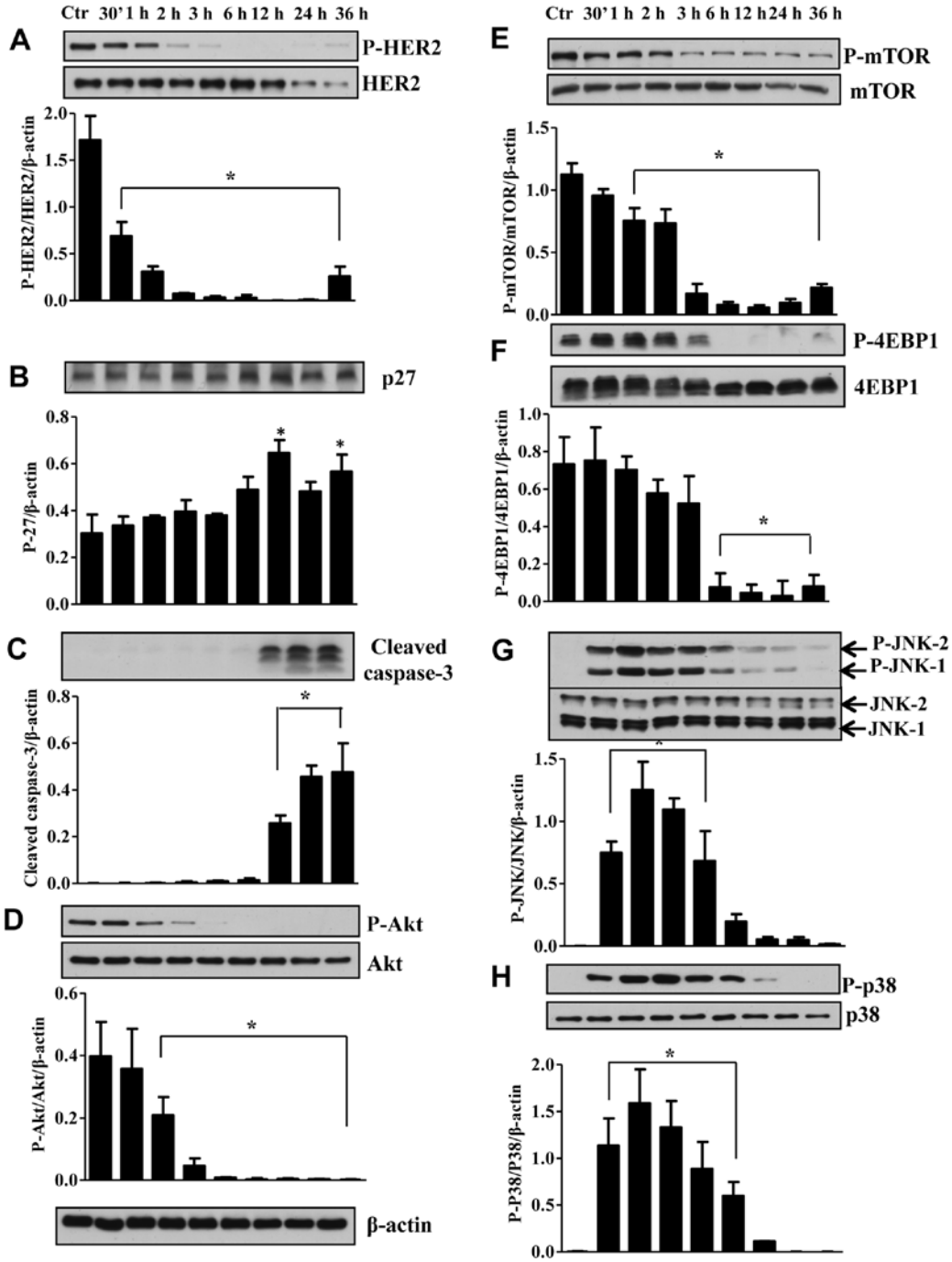

Figure 5. RL66 downregulates HER2/neu and key cell signaling proteins in SKBr3 cells. SKBr3 cells were seeded in 10-cm culture dishes at 2.5x10^6 cells per well and were treated with RL66 (2 μM) or control (0.1 % DMSO) for the indicated time. Cell lysates were then prepared, and the expression of (A) HER2/neu, (B) p27 and (C) cleaved caspase-3, (D) Akt, (E) mTOR, (F) 4EBP1, (G) JNK1/2 and (H) p38 were examined using western immunoblotting. Bars represent the mean ± SEM from 3 independent experiments. Representative blots are shown above each bar graph. Data were analyzed using a two-way ANOVA coupled with a Bonferroni post hoc test. *indicates significantly different from control, $p<0.05$.

2-24 h (Fig. 5A). To link the changes in HER2/neu with cell cycle progression protein changes in the cyclin dependent kinase inhibitor, p27 were determined. The results showed that decrease in HER2/neu correlated with a significant increase in the expression of p27 at 12 and 36 h (Fig. 5B). Thus the decrease in HER2/neu leads to an increase in p27 leading to the observed G2/M arrest and apoptosis. The presence of apoptosis was also confirmed in SKBr3 cells by the signficant increase in cleaved caspase-3 (Fig. 5C). Proteins downstream of EGFR were also examined and RL66 treatment resulted in a 90% decrease in the ratio of pAkt/Akt (Fig. 5D). This correlated with a decrease in mTOR and its downstream effector 4EBP1 (Fig. 5E and F). Conversely, the stress kinases JNK1/2 and p38 were transiently incrased from 30 min-6 h (Fig. 5G and H). Thus, RL66 produces a consistent time-dependent disruption of cell signaling proteins in SKBr3 cells that begins with potent inhibition of HER2/neu.

To determine the molecular mechanisms responsible for apoptosis and cell cycle arrest in TNBC cells we first exam-

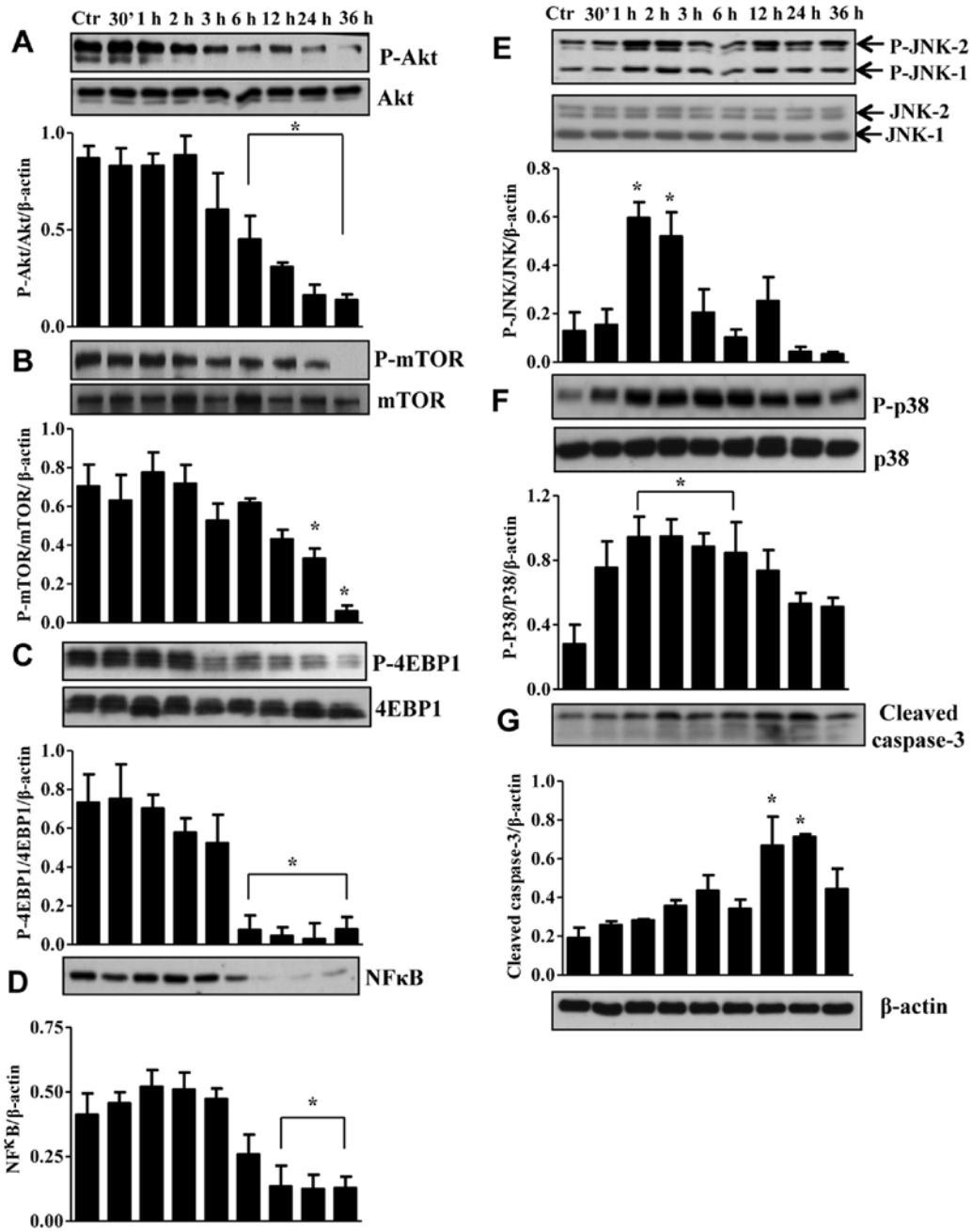

Figure 6. RL66 modulates cell signaling proteins in MDA-MB-231 cells. MDA-MB-231 cells were seeded in 10-cm culture dishes at $2.5x10^6$ cells per well and were treated with RL66 (2 μM) or control (0.1 % DMSO) for the indicated time. Cell lysates were then prepared, and the expression of (A) Akt, (B) mTOR, (C) 4EBP1, (D) NF-κB, (E) JNK1/2, (F) p38 and (G) cleaved caspase-3 were examined using western immunoblotting. Bars represent the mean ± SEM from 3 independent experiments. Representative blots are shown above each bar graph. Data were analyzed using a two-way ANOVA coupled with a Bonferroni post hoc test. *indicates significantly different from control, $p<0.05$.

ined for other isoforms of the EGFR. RL66 failed to alter the ratio of pEGFR/EGFR protein levels (data not shown). However, RL66 did modulate the expression of Akt, mTOR, 4EBP1, NF-κB, JNK1/2, p38 and caspase-3 in MDA-MB-231 (Fig. 6) and Akt, mTOR, p27, JNK1/2, p38 and caspase-3 in MDA-MB-468 cells (Fig. 7). Specifically, RL66 significantly decreased the ratio of pAkt/Akt from 6-36 h in MDA-MB-231 cells and at 36 h in MDA-MB-468 cells (Figs. 6A and 7A). The stress initiated by the treatment of MDA-MB-231 and MDA-MB-468 cells resulted in a transient increase in both JNK1/2 and p38 MAPK phosphorylation (Figs. 6E, F and 7D, E). Furthermore, RL66 increased levels of cleaved caspase 3 at 12 and 24 h (Figs. 6G and 7F). MDA-MB-231 cells were the only cell line to show a signficant decrease in NF-κB which occurred at 12-36 h (Fig. 6D).

To determine if RL66 could modulate angiogenesis, *in vitro* assays using HUVEC cells were performed, as the ability of these cells to migrate through matrigel and their ability to form tube-like networks are hallmarks of angiogenesis. Quantifiable and visual assys were used to form a more complete *in vitro* picture. The results showed that RL66 (1 μM) significantly reduced HUVEC cell migration by 46% compared to vehicle

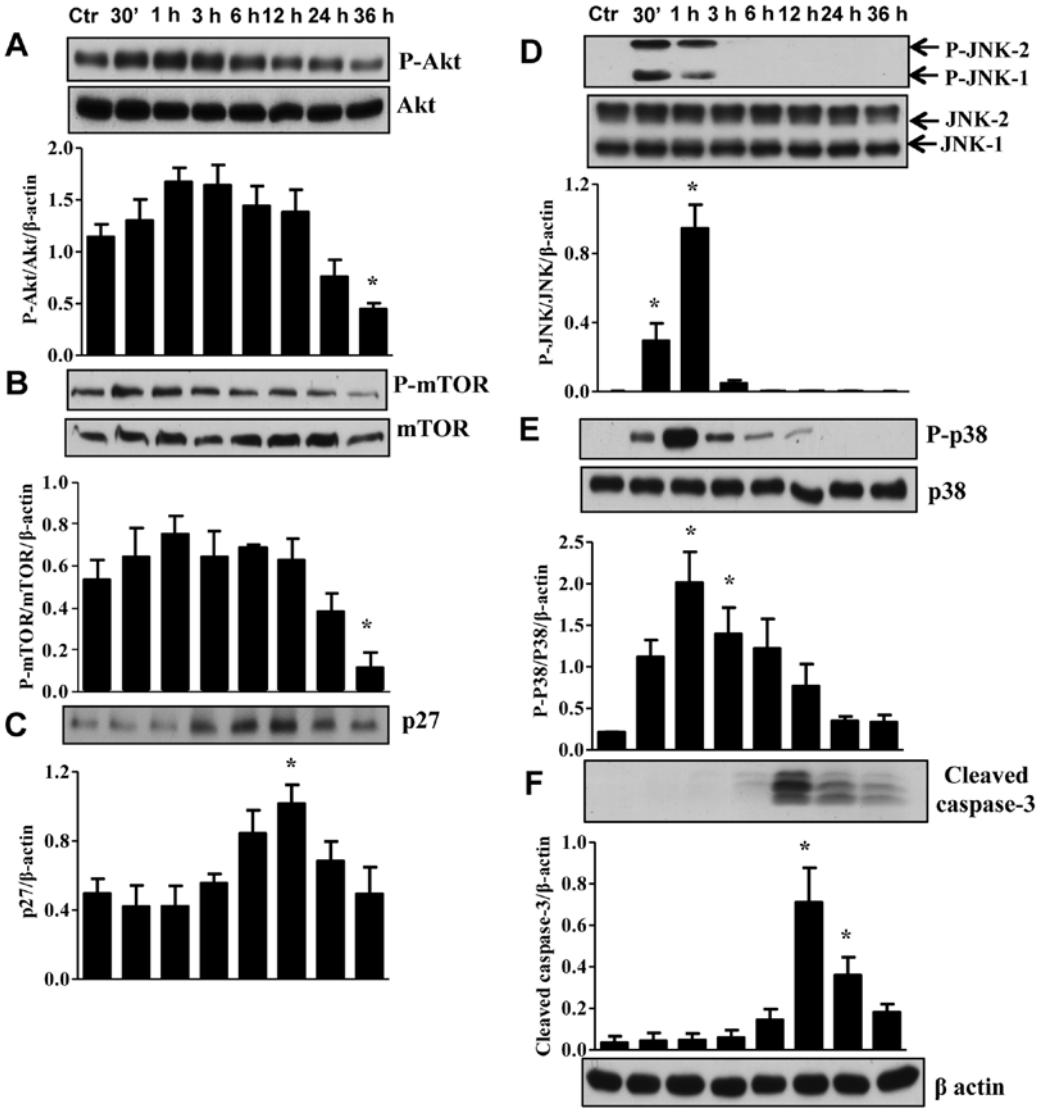

Figure 7. RL66 modulates cell signaling proteins in MDA-MB-468 cells. MDA-MB-468 cells were seeded in 10-cm culture dishes at 2.5x10^6 cells per well and were treated with RL66 (3 μM) or control (0.1 % DMSO) for the indicated time. Cell lysates were then prepared, and the expression of (A) Akt, (B) mTOR, (C) p27, (D) JNK1/2, (E) p38 and (F) cleaved caspase-3 were examined using western immunoblotting. Bars represent the mean ± SEM from 3 independent experiments. Representative blots are shown above each bar graph. Data were analyzed using a two-way ANOVA coupled with a Bonferroni post hoc test. *indicates significantly different from control, $p<0.05$.

control (Fig. 8A) and completely inhibited endothelial tube formation (Fig. 8B).

To determine if these potent *in vitro* effects would translate to *in vivo* tumor suppression, RL66 was examined for its ability to modulate tumor growth in a xenograft model of TNBC. The results showed that tumors in mice treated with RL66 (8.5 mg/kg) were significantly smaller in volume compared to tumors from vehicle treated mice (Fig. 9A). This effect was apparent after 4 weeks of treatment and continued throughout the 10 weeks of treatment. At the conclusion of the study tumor volume and weight was 48% smaller in the RL66 treated mice compared to vehicle control. Importantly, RL66 treatment was non-toxic to the mice as body weight, gross organ weight of the liver, kidney, spleen and uterus was not different between treatment and control (data not shown). Additionally, plasma alanine aminotransferase activity, a marker of hepatotoxicity, remained in the normal range (23-85 IU/l). To determine if the tumor suppression elicited by RL66 was accompanied with a decrease in microvessel density, tumors were sectioned and stained for the blood vessel marker CD105. The results demonstrated that RL66 (8.5 mg/kg) significantly decreased CD105 staining 57% compared to control tumors (Fig. 9B and C).

Discussion

We have previously shown that RL66 elicited high cytotoxic potency towards ER-negative breast cancer cells (20). Therefore, this study was designed to further characterize this cytotoxic effect *in vitro* and *in vivo*. The results show that RL66 promoted G2/M cell cycle arrest, induced apoptosis and modulated the Akt-dependent signaling pathway and stress response MAPK pathway. RL66 also downregulated the expression of HER2/neu in SKBr3 cells. Importantly, RL66 suppressed tumor growth *in vivo*, while it remained non-toxic to major organs. In addition,

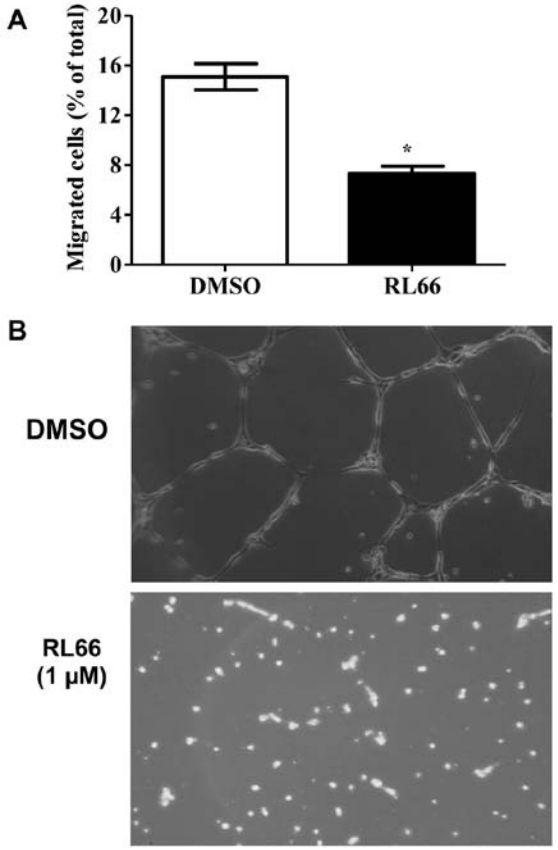

Figure 8. RL66 decreases HUVEC cell migration and tube formation. (A) HUVEC cells (25,000/well) were seeded and treated with either DMSO (0.1 %) or RL66 (1 μM) for 18 h. Migrated cells were stained and counted. Bars represent mean ± SEM of 3 independent experiments performed in triplicate. *Significantly different compared to control, p<0.01, as determined from a Student's t-test. (B) HUVEC cells (50,000/well) were seeded and treated with DMSO (0.1 %) or RL66 (1 μM) for 18 h. Photographs were then taken by an examiner blinded to the treatment groups. Representative photos from an experiment performed in quadriuplicate are shown.

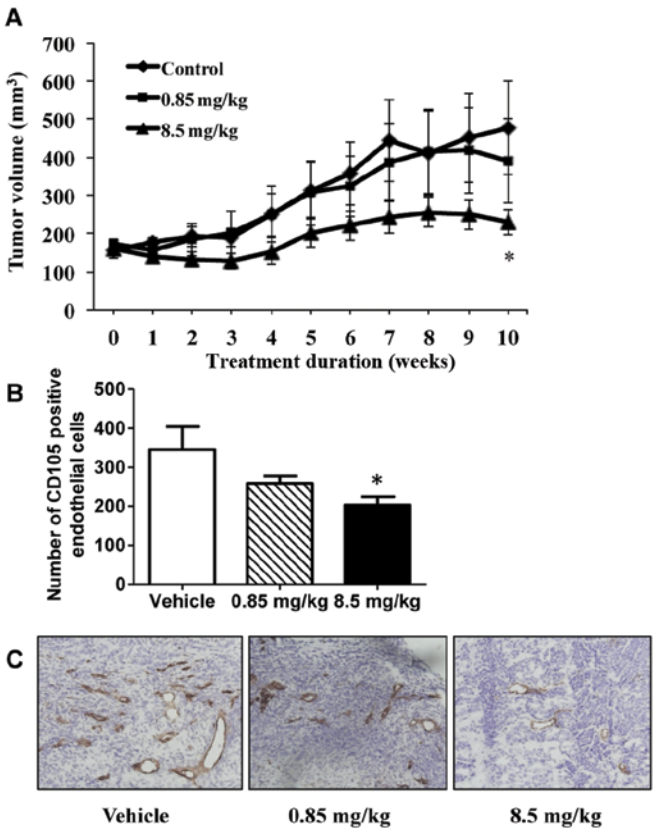

Figure 9. RL66 suppresses tumor growth and decreases tumor microvessel density. (A) MDA-MB-468 cells were injected sucutaneously into the flank of female athyic nude mice. Once tumors reached 100 mm^3 mice were randomly assigned to the treatment groups (5/group) and were dosed daily with vehicle (water), or RL66 at 8.5 mg/kg or 0.85 mg/kg for 10 weeks. Symbols represent the mean ± SEM. *Significantly different compared to control, p<0.01, as determined from a repeated measures 2-way ANOVA coupled with a Bonferroni post hoc test. (B) Number of CD105 positive endothelial cells in tumor sections from treated mice. Bars represent mean ± SEM. *Significantly different compared to control, p<0.01, as determined from a one-way ANOVA coupled with a Bonferroni post hoc test. (C) Representative immunohistochemistry of CD105 staining from tumor sections of treated mice. Photographs were then taken by an examiner blinded to the treatment groups. Representative photos from sections taken from each tumor are shown.

RL66 exhibited anti-angiogenic effects *in vitro* by inhibiting the invasion of HUVEC cells and their ability to form endothelial tube-like network and *in vivo* by decreasing microvessel density in tumor slices.

RL66 displays potent cytotoxicity in ER-negative breast cancer cells compared to other cyclohexanone curcumin analogs (18,20). Moreover, it had superior cytotoxicity compared with other curcumin analogs such as 3,5-bis(flurobenzylidene) piperidin-4-one (EF24) (26), 5-bis (4-hydroxy-3-methoxy-benzylidnen)-N-methyl-4-piperidone (PAC) (27) and GO-Y030 (28) in MDA-MB-231 cells. Specifically IC_{50} values of 1.2, 1 and 0.3 μM were reported for EF24, GO-Y030 and RL66, respectively (20,26,28). While EF24 induced G2/M phase arrest and apoptosis in MDA-MB-231 cells (19) and inhibited the NF-κB pathway in a TNFα-dependent manner (26), it has not been examined in other breast cancer cells. Additionally, RL66 has a stronger ability to induce apoptosis compared to the analog 4-hydroxy-3-methoxybenzoic acid methyl ester (HM-BME), where 25 μM was required to cause 37% of LNCaP prostate cancer cells to undergo apoptosis after 24 h (29). The curcumin analogs FLLL11 and FLLL12 were equally potent as RL66 in MDA-MB-468 cells with similar IC_{50} values (0.3 μM). However, this did not translate to other breast cancer cell types as these analogs had IC_{50}s of 2-5 μM in MDA-MB-231 and SkBr3 cells (27). These analogs also downregulated Akt phosphorylation and HER2/neu expression in SKBr3 breast cancer cells but at concentrations of 10 μM, 5-fold greater than RL66 (30). Overall RL66 is more potent as all of its anticancer actions were elicited at concentrations of 3 μM or less.

Breast cancer patients whose tumors overexpress HER2/neu have a poor prognosis, shorter relapse time and lower survival time (31). In this study we showed that RL66 decreased HER2/neu expression in SKBr3 cells, which led to a decrease in Akt and mTOR as well as an increase in p27 and cleaved caspase-3. Since p27 is a key regulator of G2/M phase arrest and apoptosis (32,33), inhibition of HER2/neu is a key initial mechanism for the apoptotoic effect elicited by RL66 in SKBr3 cells. RL66 was more potent than some curcumin analogs at down-regulating the expression of HER2/neu, as 4 μM concentrations of RL90 and RL91 and 10 μM concentrations of and FLLL11

and FLLL12, were required to elicit a similar effect (30,34). However, it was not more effective than RL71, which inhibited HER2/neu at 1 μM (21). However, RL66 remains a strong drug candidate for ER-negative/HER2-positive breast cancer, especially since it has shown efficacy *in vivo*, which to date RL71 has not displayed (21).

MAPK signaling which includes activation of JNK and p38 is involved in the regulation of the cell cycle and induction of apoptosis in breast cancer cells (35). Various cytotoxic agents induce apoptotic cell death via activation of MAPK signaling and induction of caspase-3 (36-38). Our studies showed that RL66 treatment induced JNK1/2 and p38 MAPK in MDA-MB-231 and MDA-MB-468 cells. Anticancer agents such as curcumin, which causes activation of p38, JNK1/2 and caspase-3, also induce similar apoptotic events (39,40). The MAPK pathway may also upregulate the cell cycle regulatory protein, p27 in breast cancer cells (41). Our results demonstrated that in MDA-MB-468 RL66 enhanced the expression of p27 which would contribute to the observed G2/M cell cycle arrest.

We further studied the effect of RL66 on the PI3K/Akt/mTOR pathway. Akt is an important oncoprotein which is constitutively active in breast cancer cells and has been implicated in numerous regulatory mechanisms involving protein synthesis, cell cycle progression and inhibition of apoptosis (42,43). Our results showed that RL66 decreased the phosphorylation of Akt on Ser-473 in a cell line and time-dependent manner. Specifically, in MDA-MB-231 cells, RL66 decreased Akt phosphorylation after 6 h whereas in MDA-MB-468 cells the phosphorylation of Akt was only decreased after 36 h. However, RL66 was more potent than the analogs RL90 and RL91, which did not decrease the ratio of pAkt/Akt at concentrations of 4 μM (34). The decreased activity of Akt led to decreased activation of its substrate mTOR in both cell lines.

Akt contributes to the activity of NF-κB by controling its translocation to the nucleus (44) and a decrease in Akt activity may affect the stability and level of NF-κB (45). NF-κB belongs to a family of transcription factors which has been associated with inhibition of apoptosis by promoting the expression of anti-apoptotic proteins such as Bcl-xL, c-Myb and caspase inhibitors (46,47). RL66 downregulated the expression of NF-κB in MDA-MB-231 cells. However, higher concentrations were required to downregulate NF-κB in MDA-MB-468 cells (data not shown) and this is consistent with other curcumin analogs (21,23). Curcumin has also been shown to interfere with the functions of Akt and MAPKs and to inhibit its downstream target NF-κB (48,49) and thus RL66 retains many of the same actions as curcumin.

Importantly, the potent *in vitro* actions of RL66 translated to tumor suppression in a xenograft model of TNBC. Tumor suppression was accompanied by a 57% decrease in tumor microvessel density. While other 2nd generation heterocyclic cyclohexanone curcumin derivatives have shown potent *in vitro* actions, RL66 is the first drug in this class to elicit tumor suppression *in vivo*. This provides evidence for the need to continue examining this class of curcumin analogs.

In summary, we showed that RL66 causes cell cycle arrest and induces apoptosis in ER-negative breast cancer cells and also modulates a variety of signaling pathways that culminate in potent cytotoxicity. Specifically, inhibition of Akt pathway and the activation of p38/JNK pathway may contribute to the anticancer activity of RL66 in TNBC cells, while inhibition of HER2/neu and induction of p27 are key mechanisms in SKBr3 cells. RL66 suppresses tumor growth in an *in vivo* model of TNBC and this correlates with a decrease in tumor microvessel density. This anti-angiogenic effect was also shown *in vitro*. Thus, RL66 shows potential as a new drug therapy for ER-negative breast cancer that warrants further investigation.

Acknowledgements

This study was supported by a grant from the Breast Cancer Cure Research Trust (RJR) and a University of Otago postgraduate scholarship (BY).

References

1. Parl FF, Schmidt BP, Dupont WD and Wagner RK: Prognostic significance of estrogen receptor status in breast cancer in relation to tumor stage, axillary node metastasis, and histopathologic grading. Cancer 54: 2237-2242, 1984.
2. Doane AS, Danso M, Lal P, Donaton M, Zhang L, Hudis C and Gerald WL: An estrogen receptor-negative breast cancer subset characterized by a hormonally regulated transcriptional program and response to androgen. Oncogene 25: 3994-4008, 2006.
3. Chiu TL and Su CC: Curcumin inhibits proliferation and migration by increasing the Bax to Bcl-2 ratio and decreasing NF-κBp65 expression in breast cancer MDA-MB-231 cells. Int J Mol Med 23: 469-475, 2009.
4. Kang HJ, Lee SH, Price JE and Kim LS: Curcumin suppresses the paclitaxel-induced nuclear factor-kappaB in breast cancer cells and potentiates the growth inhibitory effect of paclitaxel in a breast cancer nude mice model. Breast J 15: 223-229, 2009.
5. Liu Q, Loo WT, Sze SC and Tong Y: Curcumin inhibits cell proliferation of MDA-MB-231 and BT-483 breast cancer cells mediated by down-regulation of NFkappaB, cyclinD and MMP-1 transcription. Phytomed 16: 916-922, 2009.
6. Prasad CP, Rath G, Mathur S, Bhatnagar D and Ralhan R: Potent growth suppressive activity of curcumin in human breast cancer cells: modulation of Wnt/beta-catenin signaling. Chem Biol Interact 181: 263-271, 2009.
7. Rowe DL, Ozbay T, O'Regan RM and Nahta R: Modulation of the BRCA1 protein and induction of apoptosis in triple negative breast cancer cell lines by the polyphenolic compound curcumin. Breast Cancer (Auckl) 3: 61-75, 2009.
8. Somers-Edgar TJ, Scandlyn MJ, Stuart EC, Le Nedelec MJ, Valentine SP and Rosengren RJ: The combination of epigallocatechin gallate and curcumin suppresses ER alpha-breast cancer cell growth in vitro and in vivo. Int J Cancer 122: 1966-1971, 2008.
9. Wu X and Wu K: Antiproliferative effect of curcumin on human breast cancer of MCF-7 cells. Di-San Junyi Daxue Xuebao 28: 1870-1872, 2006.
10. Anand P, Thomas Sherin G, Kunnumakkara Ajaikumar B, *et al*: Biological activities of curcumin and its analogues (Congeners) made by man and Mother Nature. Biochem Pharmacol 76: 1590-1611, 2008.
11. Cheng AL, Hsu CH, Lin JK, *et al*: Phase I clinical trial of curcumin, a chemopreventive agent, in patients with high-risk or pre-malignant lesions. Anticancer Res 21: 2895-2900, 2001.
12. Inano H, Onoda M, Inafuku N, *et al*: Chemoprevention by curcumin during the promotion stage of tumorigenesis of mammary gland in rats irradiated with gamma-rays. Carcinogenesis 20: 1011-1018, 1999.
13. Pereira MA, Grubbs CJ, Barnes LH, *et al*: Effects of the phytochemicals, curcumin and quercetin, upon azoxymethane-induced colon cancer and 7,12-dimethylbenz[a] anthracene-induced mammary cancer in rats. Carcinogenesis 17: 1305-1311, 1996.
14. Schaaf C, Shan B, Buchfelder M, *et al*: Curcumin acts as antitumorigenic and hormone-suppressive agent in murine and human pituitary tumour cells in vitro and in vivo. Endocr Relat Cancer 16: 1339-1350, 2009.

15. Singletary K, MacDonald C, Wallig M and Fisher C: Inhibition of 7,12-dimethylbenz[a]anthracene (DMBA)-induced mammary tumorigenesis and DMBA-DNA adduct formation by curcumin. Cancer Lett 103: 137-141, 1996.
16. Liang G, Shao L, Wang Y, *et al*: Exploration and synthesis of curcumin analogues with improved structural stability both in vitro and in vivo as cytotoxic agents. Bioorg Med Chem 17: 2623-2631, 2009.
17. Markaverich BM, Schauweker TH, Gregory RR, Varma M, Kittrell FS, Medina D and Varma RS: Nuclear type II sites and malignant cell proliferation: inhibition by 2,6-bis-benzylidene-cyclohexanones. Cancer Res 52: 2482-2488, 1992.
18. Adams BK, Ferstl EM, Davis MC, *et al*: Synthesis and biological evaluation of novel curcumin analogs as anti-cancer and anti-angiogenesis agents. Bioorg Med Chem 12: 3871-3883, 2004.
19. Adams BK, Cai J, Armstrong J, *et al*: EF24, a novel synthetic curcumin analog, induces apoptosis in cancer cells via a redox-dependent mechanism. Anticancer Drugs 16: 263-275, 2005.
20. Yadav B, Taurin S, Rosengren RJ, Schumacher M, Diederich M, Somers-Edgar TJ and Larsen L: Synthesis and cytotoxic potential of heterocyclic cyclohexanone analogues of curcumin. Bioorg Med Chem 18: 6701-6707, 2010.
21. Yadav B, Taurin S, Larsen L and Rosengren RJ: RL71, a second-genration curcumin analog, induces apoptosis and downregulates Akt in ER-negative breast cancer cells. Int J Oncol 41: 1119-1127, 2012.
22. Skehan P, Storeng R, Scudiero D, *et al*: New colorimetric cytotoxicity assay for anti-cancer drug screening. J Natl Cancer Inst 82: 1107-1112, 1990.
23. Somers-Edgar TJ, Taurin S, Larsen L, Chandramouli A, Nelson MA and Rosengren RJ: Mechanisms for the activity of heterocyclic cyclohexanone curcumin derivatives in estrogen receptor negative human breast cancer cell lines. Invest New Drugs 29: 87-97, 2011.
24. Stuart EC and Rosengren RJ: The combination of raloxifene and epigallocatechin gallate suppresses growth and induces apoptosis in MDA-MB-231 cells. Life Sci 82: 943-948, 2008.
25. Smith PK, Krohn RI, Hermanson GT, *et al*: Measurement of protein using bicinchoninic acid. Anal Biochem 150: 76-85, 1985.
26. Kasinski AL, Du Y, Thomas SL, *et al*: Inhibition of IkappaB kinase-nuclear factor-kappaB signaling pathway by 3,5-bis(2-flurobenzylidene)piperidin-4-one (EF24), a novel monoketone analog of curcumin. Mol Pharmacol 74: 654-661, 2008.
27. Al-Hujaily EM, Mohamed AG, Al-Sharif I, *et al*: PAC, a novel curcumin analogue, has anti-breast cancer properties with higher efficiency on Er-negative cells. Breast Cancer Res Treat 128: 97-107, 2011.
28. Hutzen B, Friedman L, Sobo M, *et al*: Curcumin analogue GO-Y030 inhibits STAT3 activity and cell growth in breast and pancreatic carcinomas. Inter J Oncol 35: 867-872, 2009.
29. Kumar AP, Garcia GE, Ghosh R, Rajnarayanan RV, Alworth WL and Slaga TJ: 4-Hydroxy-3-methoxybenzoic acid methyl ester: a curcumin derivative targets Akt/NF kappa B cell survival signaling pathway: potential for prostate cancer management. Neoplasia 5: 255-266, 2003.
30. Lin L, Hutzen B, Ball S, *et al*: New curcumin analogues exhibit enhanced growth-suppressive activity and inhibit AKT and signal transducer and activator of transcription 3 phosphorylation in breast and prostate cancer cells. Cancer Sci 100: 1719-1727, 2009.
31. Wang SC and Hung MC: HER2 overexpression and cancer targeting. Semin Oncol 28: 115-124, 2001.
32. Hsieh WT, Huang KY, Lin HY and Chung JG: *Physalis angulata* induced G2/M phase arrest in human breast cancer cells. Food Chem Toxicol 44: 974-983, 2006.
33. Hsu JD, Kao SH, Ou TT, Chen YJ, Li YJ and Wang CJ: Gallic acid induces G2/M phase arrest of breast cancer cell MCF-7 through stabilization of p27(Kip1) attributed to disruption of p27(Kip1)/Skp2 complex. J Agric Food Chem 59: 1996-2003, 2011.
34. Somers-Edgar TJ, Taurin S, Larsen L, Chandramouli A, Nelson MA and Rosengren RJ: Mechanisms for the activity of heterocyclic cyclohexanone curcumin derivatives in estrogen receptor negative human breast cancer cell lines. Invest New Drugs 29: 87-97, 2011.
35. Santen RJ, Song RX, McPherson R, Kumar R, Adam L, Jeng MH and Yue W: The role of mitogen-activated protein (MAP) kinase in breast cancer. J Steroid Biochem Mol Biol 80: 239-256, 2002.
36. Wada T and Penninger JM: Mitogen-activated protein kinases in apoptosis regulation. Oncogene 23: 2838-2849, 2004.
37. Liu B, Han M, Sun RH, Wang JJ, Zhang YP, Zhang DQ and Wen JK: ABL-N-induced apoptosis in human breast cancer cells is partially mediated by c-Jun NH2-terminal kinase activation. Breast Cancer Res 12: R9, 2010.
38. Kuo PL, Chen CY and Hsu YL: Isoobtusilactone A induces cell cycle arrest and apoptosis through reactive oxygen species/apoptosis signal-regulating kinase 1 signaling pathway in human breast cancer cells. Cancer Res 67: 7406-7420, 2007.
39. Collett GP and Campbell FC: Curcumin induces c-jun N-terminal kinase-dependent apoptosis in HCT116 human colon cancer cells. Carcinogenesis 25: 2183-2189, 2004.
40. Weir NM, Selvendiran K, Kutala VK, *et al*: Curcumin induces G2/M arrest and apoptosis in cisplatin-resistant human ovarian cancer cells by modulating Akt and p38 MAPK. Cancer Biol Ther 6: 178-184, 2007.
41. Eto I: Nutritional and chemopreventive anti-cancer agents up-regulate expression of p27Kip1, a cyclin-dependent kinase inhibitor, in mouse JB6 epidermal and human MCF7, MDA-MB-321 and AU565 breast cancer cells. Cancer Cell Int 6: 20, 2006.
42. Dillon RL, White DE and Muller WJ: The phosphatidyl inositol 3-kinase signaling network: implications for human breast cancer. Oncogene 26: 1338-1345, 2007.
43. Vivanco I and Sawyers CL: The phosphatidylinositol 3-Kinase AKT pathway in human cancer. Nat Rev Cancer 2: 489-501, 2002.
44. Burow ME, Weldon CB, Melnik LI, Duong BN, Collins-Burow BM, Beckman BS and McLachlan JA: PI3-K/AKT regulation of NF-kappaB signaling events in suppression of TNF-induced apoptosis. Biochem Biophys Res Commun 271: 342-345, 2000.
45. Gong L, Li Y, Nedeljkovic-Kurepa A and Sarkar FH: Inactivation of NF-kappaB by genistein is mediated via Akt signaling pathway in breast cancer cells. Oncogene 22: 4702-4709, 2003.
46. Barkett M and Gilmore TD: Control of apoptosis by Rel/NF-kappaB transcription factors. Oncogene 18: 6910-6924, 1999.
47. Lauder A, Castellanos A and Weston K: c-Myb transcription is activated by protein kinase B (PKB) following interleukin 2 stimulation of T cells and is required for PKB-mediated protection from apoptosis. Mol Cell Biol 21: 5797-5805, 2001.
48. Shehzad A, Wahid F and Lee YS: Curcumin in cancer chemoprevention: molecular targets, pharmacokinetics, bioavailability, and clinical trials. Arch Pharm (Weinheim) 343: 489-499, 2010.
49. Dhandapani KM, Mahesh VB and Brann DW: Curcumin suppresses growth and chemoresistance of human glioblastoma cells via AP-1 and NFkappaB transcription factors. J Neurochem 102: 522-538, 2007.